Available online at www.sciencedirect.com
ScienceDirect
Journal of Catalysis 251 (2007) 474–484
JOURNAL OF CATALYSIS
www.elsevier.com/locate/jcat

Low-temperature propene combustion over Pt/K-βAl_2O_3 electrochemical catalyst: Characterization, catalytic activity measurements, and investigation of the NEMCA effect

Antonio de Lucas-Consuegra [a], Fernando Dorado [a], José Luis Valverde [a], Reda Karoum [b], Philippe Vernoux [b,*]

[a] *Departamento de Ingeniería Química, Facultad de Ciencias Químicas, Universidad de Castilla-La Mancha, Avenida Camilo José Cela 10, 13071 Ciudad Real, Spain*

[b] *Université de Lyon, Institut de Recherches sur la Catalyse et l'Environnement de Lyon, UMR 5256, CNRS, Université Lyon 1, 69626 Villeurbanne, France*

Received 6 April 2007; revised 22 June 2007; accepted 27 June 2007

Abstract

Studies of characterization and electrochemical promotion of the electrochemical catalyst Pt/K-βAl_2O_3 for low-temperature propene combustion are reported for the first time. Characterization of Pt/K-βAl_2O_3 by surface titration, SEM, and XRD revealed useful information about the electrochemical catalyst. On the other hand, it was found that Pt/K-βAl_2O_3 can be strongly promoted at low temperature for propene oxidation under both near-stoichiometric and oxygen-rich conditions. For instance, under C_3H_6/O_2: 2000 ppm/7% at 200 °C, a rate enhancement ratio (ρ_{CO_2}) of 7 was achieved under application of $V_{WR} = -2$ V, increasing propene conversion from 10 to 70%. In addition, the origin of the NEMCA effect was investigated using cyclic voltammetry along with CO_2 analysis as well as FTIR measurements and SEM-EDX analysis. These techniques showed that the presence of more stable and effective promoter phases (potassium oxides and superoxides) were responsible for both a permanent NEMCA effect and a higher promotional phenomenon in comparison to sodium conductors.

Keywords: Electrochemical promotion; NEMCA effect; Propene combustion; VOCs abatement; Pt catalyst; Permanent NEMCA effect

1. Introduction

Catalytic combustion of hydrocarbons is a nonpolluting means of heat generation and also may be used to destroy volatile organic contaminants (VOCs) present at trace levels in large amounts of oxygen (e.g., automotive exhaust). The most effective catalysts for the catalytic combustion of light hydrocarbons (methane, propane, or propene) are supported noble metals, such as platinum [1]. However, these kinds of catalysts are very expensive and thus require various stages of recovery and recycling. Alternately, the use of electrochemistry to activate and control a reaction process is an expanding domain, because it allows for significantly improved catalytic performance of metal catalysts by reducing the energy requirements (to work at lower temperatures) or the amount of metal (to use thinner films). This process, called the non-Faradaic electrochemical modification of catalytic activity (NEMCA) effect, or electrochemical promotion of catalysis (EPOC), was discovered [2] and developed [3,4] by Vayenas and co-workers. It is based on the control, by an applied potential, of the catalyst work function due to electrochemical pumping of ions (promoters) from a solid electrolyte [5,6]. Recent studies have explored the utility of electrochemical promotion to improve Pt catalytic activity for propene combustion using YSZ [7,8], YZTi10 [9], Na-βAl_2O_3 [10], and NASICON [11] as solid electrolytes. All of these studies were carried out at 300–500 °C, which is the usual working temperature range for an electrochemical catalyst. However, the fuel-efficient characteristics of diesel engines result in low exhaust gas temperatures (below 300 °C), espe-

---

[*] Corresponding author. Fax: +33 4 72 43 16 95.
E-mail address: philippe.vernoux@ircelyon.univ-lyon1.fr (P. Vernoux).

0021-9517/$ – see front matter
doi:10.1016/j.jcat.2007.06.031

cially during low-speed driving. This implies that the practical development of EPOC for car exhaust treatment depends on new electrochemical catalysts (i.e., coupling catalysts and solid electrolytes) able to work at lower temperatures with high efficiency. Concerning the catalyst, we have recently shown [12] that the wet-impregnation procedure is a suitable and simple technique for preparing Pt catalyst films with reasonable Pt dispersion that are active at lower temperatures. Regarding solid electrolytes, sodium conductors such as NASICON and Na-βAl_2O_3 have higher ionic conductivities at lower temperatures than anionic ones, such as YSZ or CGO. Unfortunately, previous studies have shown that electropumping of Na ions from Na-βAl_2O_3 [10] or NASICON [11] can activate Pt catalyst for propene oxidation under fuel-rich conditions, but not under oxygen-rich conditions.

The aim of our research was to find an electrochemical catalyst that can be effective and electrochemically promoted at low temperatures for the propene oxidation reaction under both near-stoichiometric (for energy production) and oxygen-rich conditions (for VOC abatement) or unburned hydrocarbon elimination in car exhaust. Potassium is known as a classical promoter [13] and has been widely used in various catalytic reactions. For instance, it has been used to promote Pt catalysts for the reduction of NO by propene [14] and for CO oxidation [15]. In addition, the electrochemical promotion by potassium on Pt catalyst has been investigated for the selective hydrogenation of acetylene [16]. This work has demonstrated the extraordinary promotional effect of potassium in improving the catalytic activity and selectivity of Pt in an even more pronounced way than Na [15]. In the present work, we studied for the first time the electrochemical promotion by potassium of Pt catalyst for low-temperature propene combustion. Our findings clearly demonstrate the practical applications of EPOC for catalytic combustion of hydrocarbons, because we have found that Pt/K-βAl_2O_3 electrochemical catalyst can be strongly promoted at low temperatures while exhibiting high catalytic performance under both near-stoichiometric and oxygen-rich conditions.

2. Experimental

2.1. Electrochemical catalyst preparation

The electrochemical catalyst consisted of a porous, continuous, thin Pt film (geometric area of 1.12 cm^2) deposited on a side of a 17-mm-diameter, 1-mm-thick K-βAl_2O_3 disc (Ionotec). Au counter and reference electrodes were deposited on the other side. These electrodes were deposited by applying thin coatings of gold paste (Gwent Electronic Materials C1991025D2), followed by calcination at 800 °C for 2 h. Gold was selected because it exhibits no significant activity for propene combustion in the form of large particles (1 µm diameter) under our operating conditions, as checked by blank experiments. Then the Pt film was deposited, as described in detail elsewhere [12], by successive steps of deposition and thermal decomposition (650 °C for 1 h) of an H_2PtCl_6 precursor solution, with a metal concentration of 0.1 M. The final Pt loading was 1.24 mg Pt/cm^2.

2.2. Catalytic activity measurements

Catalytic activity measurements of Pt films deposited on K-βAl_2O_3 were performed in a quartz reactor as described previously [7]. The reaction gases were mixtures of C_3H_6 (Air Liquide, 8000 ± 240 ppm), O_2 (Air Liquide, 99.95%), and He (Air Liquide, 99.999%), which was used as the vector gas. The gas composition was controlled by mass flow controllers (Brooks), with accuracy $>1\%$. The feed composition was 2000 ppm C_3H_6, 1–7% O_2, and the balance He; the overall flow rate was 4 L/h. Reactants and products were analyzed using an online micro-gas chromatograph (Varian CP-2003), whereas CO_2 concentration in the effluent from the reactor was also continuously monitored using an infrared (IR) analyzer (Horiba VA-3000). Before analysis, the water produced by the catalytic reactions was trapped by an electro-gas cooler (M&C Products, ECP1000-G).

The propene conversion into CO_2 was defined as

$$\text{propene conversion} = 100 \times P_{CO_2}/(P_{CO_2} + 3 \times P_{C_3H_6}), \qquad (1)$$

where P_{CO_2} and $P_{C_3H_6}$ are the partial pressures of CO_2 and propene in the outlet gas, respectively. Carbon dioxide was the only carbon-containing oxidation product. Carbon monoxide was not detected according to our lower detection limit of 50 ppm. The carbon mass balance between C_3H_6 and CO_2 had an error $<3\%$; therefore, we can assume that CO_2 formation from possible carbon deposition was insignificant during the catalytic tests. Before catalytic activity measurements, the Pt film was pretreated under H_2 at 450 °C for 1 h to reduce the metal. Then the sample was cooled down to 200 °C under a flow of helium. The reactive mixture flow (with 1% O_2) was switched into the reactor, and the sample was heated to 650 °C at a rate of 1 °C/min. The catalyst was maintained at 650 °C for 12 h, after which the temperature was decreased to 200 °C at a rate of 1 °C/min. This procedure aimed to stabilize the Pt film morphology and to identify the degree of catalyst durability against thermal sintering needed in catalyst formulations. The three electrodes, W (catalyst or working electrode), R (reference), and CE (counter-electrode) were connected to a Voltalab 80 potentiostat-galvanostat (Radiometer Analytical). Voltage or current was applied and measured according to the procedure generally used in conventional three-electrode electrochemical cells. The catalyst potential (V_{WR}) was measured between the working electrode (Pt) and the reference electrode (Au), which may be considered as a pseudoreference because we have checked that its potential does not vary significantly with the composition of the gaseous mixture.

2.3. Characterization measurements

The dispersion of the Pt catalyst film and its chemisorption properties at varying catalyst potential were characterized by the isothermal surface titration technique. The Pt particle size before catalysis (fresh sample) and after catalysis (aged sample) was obtained by grazing angle X-ray diffraction (XRD) ($\lambda_{K\alpha Co} = 0.179$ nm) using an Inel diffractometer with an incipient angle of 4°. The morphology and composition of the Pt film before and after catalysis were also investigated via scanning electron microscopy (SEM), using a Phillips FEG XL30S microscope equipped with an energy-dispersive X-ray analyzer (EDX). Cyclic voltammetry measurements in conjunction with CO_2 analysis were performed with a potentiostat-galvanostat Voltalab 80 (Radiometer Analytical) under different reaction conditions and recorded at a sweep rate of 2 mV/s.

In addition, to identify the state of the different potassium promoter species under reaction conditions, in situ Fourier transform infrared spectroscopy (FTIR) measurements were carried out in an IR reactor cell as described previously [17]. In situ FTIR spectra were collected with a Perkin–Elmer Spectrum GX spectrometer by accumulating 100 scans at a resolution of 4 cm^{-1}. The focused wave number range was 4000–1000 cm^{-1}. FTIR measurements were carried out over a 1% Pt/K-βAl_2O_3 powder, which simulated the Pt catalyst working electrode. It was prepared by a conventional impregnation procedure as follows. A powder of the solid electrolyte K-βAl_2O_3 (Ionotec) was impregnated with a $H_2PtCl_6^+$ solution precursor in a glass vessel under vacuum at 60 °C to yield 1% weight of Pt. After drying overnight at 120 °C, the resulting powder was calcined at 450 °C for 4 h to prepare it for precursor decomposition.

3. Results and discussion

3.1. Electrochemical catalyst characterization

The dispersion of the Pt film after catalysis was determined by measuring its reactive oxygen uptake at 350 °C via the isothermal titration technique [5]. The Pt film was first exposed to O_2 for 15 min, after which the reactor was purged with pure He for t_{He}, several times longer than the reactor residence time to remove gaseous O_2. Subsequently, the reactor was purged with C_3H_6, and the amount of oxygen remaining on the Pt surface (N) was obtained by integrating the area of the CO_2 peak in the reactor effluent. Due to the high conductivity of the solid electrolyte at 350 °C, during the isothermal titration technique, a positive catalyst potential of $V_{WR} = 2$ V was applied to avoid thermal migration of potassium ions, that could modify the chemisorption properties of the catalyst. By varying t_{He}, one can study the kinetics of oxygen desorption. By extrapolating N at $t_{He} = 0$, one obtains the reactive oxygen catalyst uptake, N_0. Fig. 1 shows the results of the surface titration measurements. The reactive oxygen uptake was $N_0 = 3.5 \times 10^{-7}$ mol O which led to a metal dispersion of 5%. This value of dispersion is higher than that typically obtained by application of coatings of metal pastes (0.5%) [4], but lower in comparison with that obtained on sputtered films (15–50%) [18]. Nevertheless, the measured value of Pt dispersion, after long term treatment at high temperature, is close to the one obtained in a typical monolithic reactor [19]. Therefore, one could envisage the use of the impregnation technique to deposit a Pt porous catalyst film onto tubes or channels, leading to a cell configuration easily adaptable to the existing catalytic devices in which EPOC could be applied, as already done with other metals [20,21].

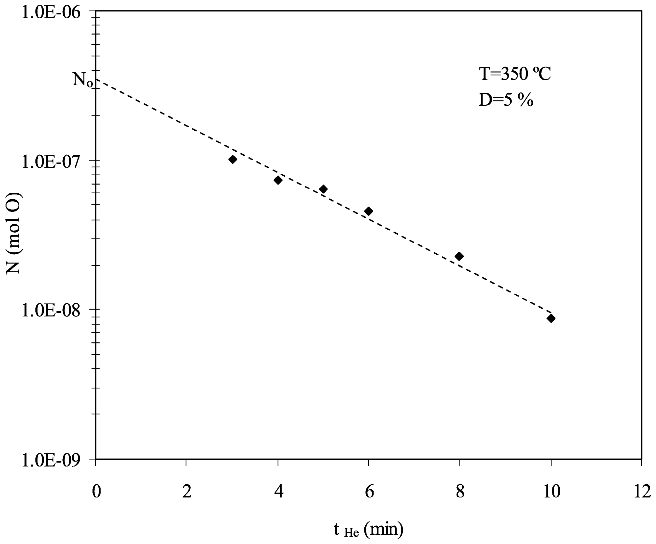

Fig. 1. Isothermal surface titration of oxygen by C_3H_6 at 350 °C. Effect of oxygen desorption time, t_{He}, on the mass of reactive oxygen adsorbed on the Pt surface.

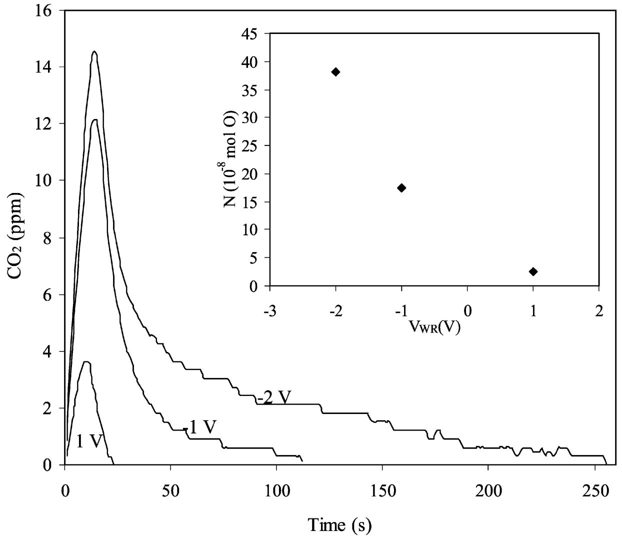

Fig. 2. Effect of the catalyst potential on CO_2 formation during the isothermal surface titration of oxygen by C_3H_6 at 250 °C. Inset: influence of the catalyst potential on the mass of reactive oxygen adsorbed on the Pt surface.

The variation of the Pt catalyst chemisorption properties at varying catalyst potential (V_{WR}) was also characterized via the isothermal titration technique. This former was carried at out at 250 °C for a constant desorption time ($t_{He} = 4$ min) under three different applied catalyst potentials. The variation of the CO_2 formation vs time during the purge with C_3H_6 for each catalyst potential is shown in Fig. 2. By integrating the area of the CO_2 peak, one can measure the oxygen remaining on the surface (N) vs the applied catalyst potential (inset Fig. 2). It can be clearly observed that as the catalyst potential decreased, the CO_2 formation during the purge with C_3H_6 as well as the width of the CO_2 peak strongly increased. Thus, as the catalyst potential decreased, there was an enhancement of the strength of the Pt–O bond during the isothermal titration experiment. It led to both an increase of the amount of oxygen remaining on the surface

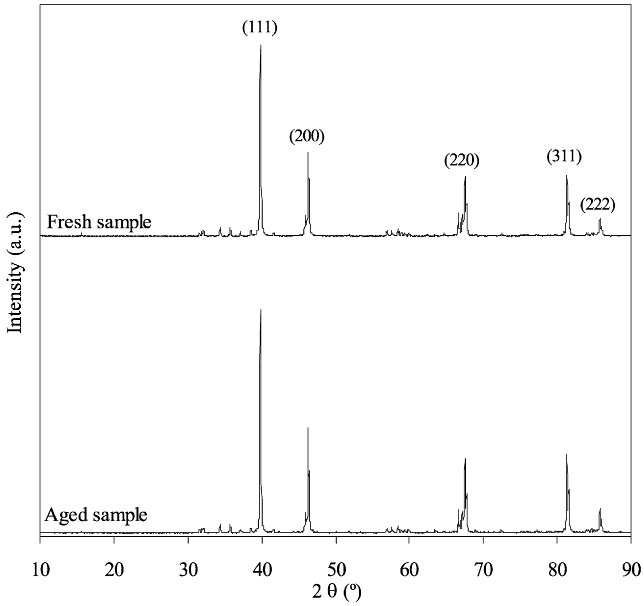

Fig. 3. Grazing angle (4°) XRD spectra of Pt catalyst before catalysis (fresh sample) and after catalysis (aged sample).

(N) after the desorption step, and a time prolongation in the CO_2 formation during the purge with propene. As already reported in previous studies [16,22–25], a decrease in the catalyst potential yields to a decrease in the catalyst work function, as the result of the transfer of positively charged potassium species on the catalyst surface, which modifies the chemisorption properties of the metal. As can be observed in Fig. 2, the presence of potassium species on the catalyst surface strongly modified the chemisorption properties of the Pt catalyst, e.g., the reactive oxygen uptake strongly increased by approximately a factor 20.

XRD patterns of the Pt catalyst-working electrode before catalysis (fresh sample) and after catalysis (aged sample) are given in Fig. 3. Peak assignments for Pt based on JCPDS standards are consistent with a face-centred cubic (fcc) structure. No pattern of platinum oxides appeared in the aged sample. This suggests that the strengthening of the Pt–O bond induced by the promoter during the catalytic experiments was not sufficient to oxidize the Pt surface. Nevertheless, a slight increase in the intensity of the diffraction peaks in the sample could be observed after catalysis. This was due to a minor sintering of Pt catalyst after long time in the reactor, which led to a small increase in the diameter of Pt particles from 55 nm in the fresh sample to 60 nm in the sample after catalysis, as measured by Scherrer's equation [26] from the analysis of the shape of the peak (111). Therefore, we can assume that the Pt film prepared by thermal decomposition of a Pt precursor solution shows significant resistance to thermal sintering, even after long treatment (12 h) at 650 °C under reaction conditions. This represents an important advantage of the wet-impregnation procedure over sputtering, because Pt-sputtered films are known to tend to sinter during reaction conditions.

Representative SEM images of the fresh (Fig. 4a) and aged (Fig. 4b) samples showed a minor sintering of the Pt agglomerates after the catalytic tests. In agreement with XRD measurements, this sintering can be considered limited, because the size of the Pt agglomerates after the catalytic test was still <1 μm. Moreover, the wet-impregnation procedure led to a very porous catalyst film, with morphology similar to those Pt films prepared by application of metal paste coatings [4], but with a much lower particle size as estimated by XRD (60 nm vs 1000 nm found previously [4]). This finding represents a unique advantage of the impregnated films, because it is well known [27] that the strength of Pt–O bonds increases as the particle size decreases. Thus, oxygen coverage on the Pt film prepared by the wet-impregnation procedure will be higher than that on catalysts prepared by application of metal pastes. Consequently, it could be active at lower temperatures, as already reported for the reduction of NO by C_3H_6 [28].

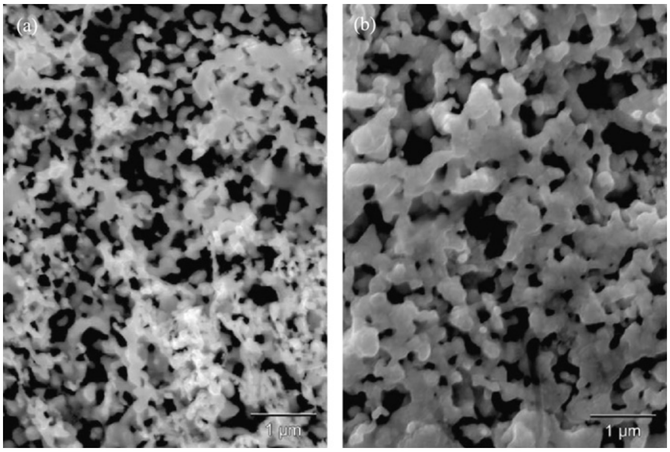

Fig. 4. Top surface SEM micrographs of the Pt catalyst film: (a) before catalysis and (b) after catalysis.

3.2. Catalytic activity measurements under near-stoichiometric oxygen conditions

We first investigated the catalytic activity of the Pt/K-βAl_2O_3 electrochemical catalyst at 270 °C under near-stoichiometric conditions, C_3H_6/O_2: 2000 ppm/1%. Fig. 5 shows the steady-state effect of the applied potential (V_{WR}) on both propene conversion and propene oxidation rate (expressed as O consumption rate, in mol O/s). In this experiment, the potentiostat was set to impose a potential difference (ΔV_{WR}) between the working and reference electrodes. Current measured between the working electrode (catalyst) and Au counterelectrode should correspond to the following cathodic reaction at the catalyst (working) electrode:

$$K^+(\beta\text{-}Al_2O_3) + e^- \rightarrow K\ (\text{catalyst}). \qquad (2)$$

This continues until the amount of K pumped from the electrolyte to the catalyst causes the value of V_{WR} to reach the desired preset value, at which point the current vanishes. It can be observed that starting from a potassium clean surface ($V_{WR} = 2$ V) and then decreasing this potential, the catalytic performance of Pt improved significantly, increasing propene conversion from 30 to 63% (Fig. 5). It should be pointed out that this is the first time that such large increase in propene conversion was found below 300 °C. As shown in Fig. 2, the variation of the catalyst work function on polarization induces changes

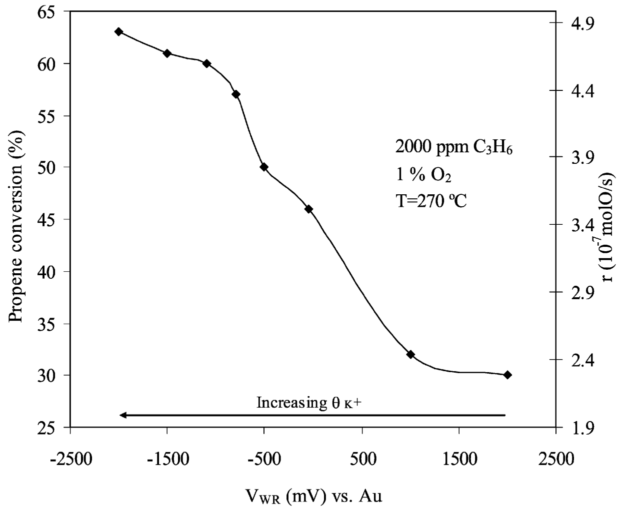

Fig. 5. Steady-state effect of applied catalyst potential (V_{WR}) on both propene conversion and catalytic reaction rate (r) expressed in mol O/s. Total flow rate = 4 L/h.

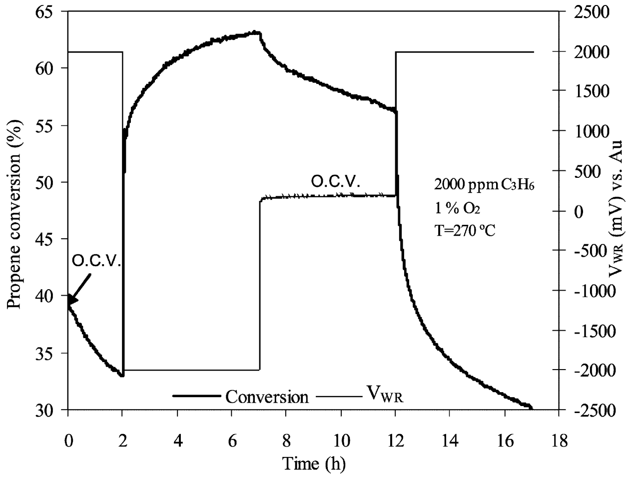

Fig. 6. Propene conversion response vs time to step changes in applied catalyst potential. Total flow rate = 4 L/h.

in the binding strength of chemisorbed species. When there is no promoter on the catalyst ($V_{WR} = 2$ V), the Pt surface is predominantly covered by propene or by propene-derived carbonaceous species [7,8]. Thus, the decreased catalyst potential enhances propene oxidation rate by increasing the coverage of electron-acceptor species (O_2) at the expense of electron-donor (C_3H_6) [8], leading to the observed electrophilic NEMCA effect. Such electrophilic NEMCA behavior has been reported for propene combustion under stoichiometric conditions for Pt catalyst deposited on Na-βAl_2O_3 [10] and NASICON [11]. Nevertheless, in these works, when the catalyst potential was decreased (<0 mV in [10] and −200 mV in [11]), a decrease in the reaction rate was also observed. This poisoning effect was attributed to the growth of three-dimensional crystallites of Na compounds (sodium carbonates) on the Pt surface that blocked the active sites. Using Pt/K-βAl_2O_3 electrochemical catalyst, we have not observed such poisoning behavior, even when the catalyst potential was decreased to lower values (−2 V) than in Refs. [10,11].

It has been suggested that this difference may be due to the lower thermal stability of bulk potassium compounds versus sodium compounds under reaction conditions, which could prevent the growth of such three-dimensional phases. To confirm this assumption, a potentiostatic transient experiment was carried out under the same reaction conditions (C_3H_6/O_2: 2000 ppm/1%; $T = 270\,^\circ C$), as shown in Fig. 6. This experiment depicts the response of the propene conversion versus time to step changes in applied potential. Initially ($t < 0$), the system was kept at open circuit conditions (OCV); later ($t = 0$), a positive potential of $V_{WR} = 2$ V was applied between the Pt catalyst and the Au reference electrode for 2 h, to clean the catalyst surface of potassium and define a reproducible state of the Pt catalyst surface. The migration of potassium ions from the Pt surface toward the K-βAl_2O_3 solid electrolyte, induced by the polarization, significantly decreased the propene conversion. Subsequent application at $t = 2$ h of a constant potential of $V_{WR} = -2$ V, with the concomitant electrochemical pumping of potassium ions to the catalyst surface, resulted in a significantly increased catalytic reaction rate, with a propene conversion value of 63%, as obtained in the previous experiment (Fig. 5). Then the circuit was opened (OCV) at $t = 7$ h, to study the stability of the promoter species. Finally, at $t = 12$ h, a catalyst potential of $V_{WR} = 2$ V was applied, to get the initial unpromoted state. The most important point is that, after the negative polarization, at $t = 7$ h, with open circuit conditions (OCV), the catalyst exhibited just a slight decrease in catalytic activity. Indeed, after 5 h, the propene conversion decreased by <10 points. This behavior, close to a permanent NEMCA effect, shows high thermal stability of the promoter species under the reaction conditions. Even after a long time at OCV (5 h), a high positive catalyst potential should be applied ($V_{WR} = 2$ V) to obtain the initial values of propene conversion.

These experiments seem to indicate that the different potentiostatic behaviors of Na^+ and K^+ conductors, with no poisoning regime in the case of K^+ cations, is not due to a lower thermal stability of potassium promoter species. Therefore, we can propose that this difference is likely due to the different nature of the promoter species formed with sodium and potassium conductors, respectively. As we show later, the nature of the potassium compounds is different from that previously reported with sodium conductors for propene oxidation [10,11]. On the other hand, two regions can be clearly distinguished in Fig. 6 under application of −2 V. The first of these leads to a very rapid increase in the catalytic reaction rate, with an instant increase in propene conversion up to 55%, whereas the second region leads to a much slower increase in propene conversion. Furthermore, after the current interruption, the rate seems to relax to a value that practically corresponds to the onset of the second region with a slower increase in conversion. This interesting behavior seems to indicate that the formation of two different promoter phases with different stabilities and promotional effects could be occurring. Therefore, we can suggest that the different nature of the promoter phases led to a higher catalytic activation for propene oxidation than that observed with sodium conductors [10,11]. This higher promotional effect of potassium can also be explained taking into account the dif-

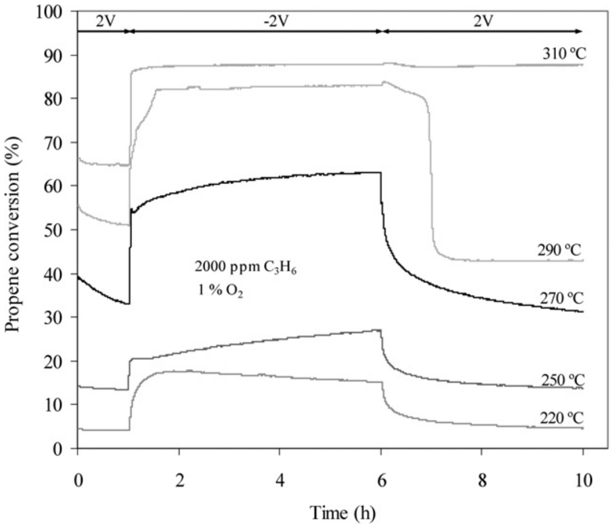

Fig. 7. Influence of the reaction temperature on the propene conversion response to step changes in applied catalyst potential vs time. Total flow rate = 4 L/h.

Table 1
Influence of the reaction temperature on the catalytic behavior and on the promotional parameters of Pt/K-βAl_2O_3 electrochemical catalysts under unpromoted ($V_{WR} = 2$ V) and promoted ($V_{WR} = -2$ V) conditions. Reaction conditions: $[C_3H_6] = 2000$ ppm, $[O_2] = 1\%$, He balance, total flow rate = 4 L/h

Temperature (°C)	r_0 (10^5 mol/s/g_{Pt})[a]	r (10^5 mol/s/g_{Pt})[b]	ρ	γ
220	0.34	1.03	3.02	1.00
250	0.99	1.87	1.88	1.00
270	2.10	4.41	2.10	1.00
290	3.01	5.86	1.95	1.00
310	4.54	6.16	1.36	1.35
E_a (kJ/mol)	69	52		

[a] (r_0) Denotes the unpromoted propene reaction rate.
[b] (r) Denotes the promoted propene reaction rate.

ferent ionic sizes of the two cations. Lang et al. [29] clearly showed that the larger the alkali cation, the greater the electric field of a co-adsorbed species located at an adjacent site. Thus, K^+ should perturb the Pt–O bond more strongly than Na^+, leading to the observed greater effectiveness of the promotional effect. This fact is in agreement with previous studies on chemical alkali promotion of Pt, CO oxidation [15], and NO reduction by C_3H_6 [14,30] and CO [31], which also showed that heavier alkalis were more effective than lighter ones.

Fig. 7 shows the response of propene conversion versus time to step changes in the applied potential, in a temperature range of 220–310 °C. First, a catalyst potential of $V_{WR} = 2$ V was applied for 1 h, then a negative polarization of $V_{WR} = -2$ V was applied for 5 h, and finally a positive potential of $V_{WR} = 2$ V was applied for 4 h, to study the reversibility of the promotional phenomenon. Table 1 summarizes the influence of the reaction temperature on both the unpromoted ($V_{WR} = 2$ V) and promoted ($V_{WR} = -2$ V) catalytic performance of Pt/K-βAl_2O_3 electrochemical catalyst and the value of the following promotional parameters [4]:

$$\text{rate enhancement ratio } (\rho) = r/r_0 \tag{3}$$

and

$$\text{permanent rate enhancement ratio } (\gamma) = r_{per}/r_0, \tag{4}$$

where r_0 is the unpromoted propene reaction rate ($t = 1$ h), r is the promoted propene reaction rate ($t = 6$ h), and r_{per} is the permanent propene reaction rate after applying 2 V for 4 h following the promoted state ($t = 10$ h).

Fig. 7 clearly shows that the application of $V_{WR} = -2$ V produced an increase in propene conversion for the entire temperature range. Thus, the system could be electrochemically promoted even at low temperatures. For instance, at 220 °C, the application of $V_{WR} = -2$ V led to a rate enhancement ratio (ρ) of 3. Therefore, it is important to note that the electrochemical promotion can be used to decrease the operation temperature of a catalyst. The effect of electrochemical pumping of potassium ions to the Pt catalyst at 270 °C led to a similar catalytic reaction rate as for the unpromoted one at 310 °C. The apparent activation energy (E_a) was also obtained via an Arrhenius-type function for the unpromoted and promoted states (Table 1). A decrease in the E_a value was found for the promoted catalyst; this could be due to the aforementioned increase in oxygen coverage on the catalyst induced by the negative polarization. Thus, we can assume that oxygen adsorption is a key step in the combustion process. The catalyst performance is strongly promoted by increased oxygen coverage. A similar decrease in activation energy under the same reaction conditions was found by Billard and Vernoux [32] on a Pt/NASICON electrochemical catalyst. These authors reported that the lower activation energy found at OCV on Pt-sputtered films ($E_a = 68$ kJ/mol) in comparison with a Pt paint sample ($E_a = 90$ kJ/mol) was due to the higher O coverage on the former (with sputtered films presenting with smaller particle sizes). On the other hand, the apparent unpromoted activation energy ($E_a = 69$ kJ/mol) of the Pt film prepared in this work is close to that found previously [32] for a Pt-sputtered film. This suggests a similar Pt particle size for both two types of catalyst films. It is also important to note that the irreversible promotional behavior begins to appear at 290 °C and is clearly observed at 310 °C (see Fig. 7). At 290 °C, it took more than 1 h with a positive potential $V_{WR} = 2$ V to see a decrease in catalytic activity. At 310 °C, the initial unpromoted catalytic rate was not achieved even when $V_{WR} = 2$ V was applied for 4 h. Therefore, at this temperature, there is a permanent NEMCA effect [33], with a permanent rate enhancement ratio of $\gamma = 1.35$ (see Table 1).

The permanent NEMCA effect is one of the most interesting and potentially important characteristics of the electrochemical promotion from a practical standpoint [4]. For instance, the permanent NEMCA effect can reduce the electrical energy requirements (polarizing the catalyst for only a short time) and lead to practical application of NEMCA during catalyst preparation. Thus, due to the theoretical and practical interest in this permanent NEMCA effect, we investigate it in detail in a separate section.

3.3. Catalytic activity measurements under oxygen-rich conditions

Fig. 8 shows the response of propene conversion versus time to step changes in catalyst potential under different oxygen-rich

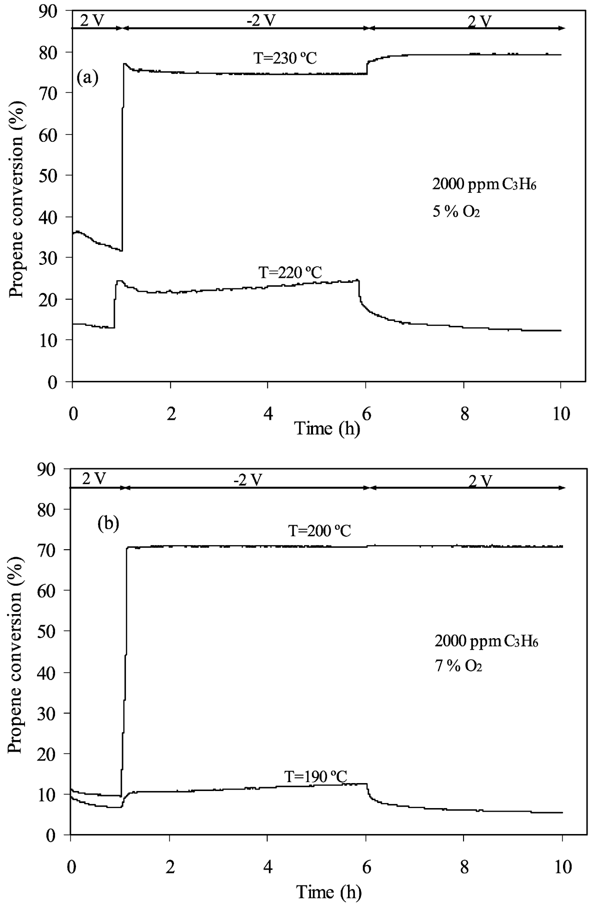

Fig. 8. Propene conversion response to step changes in applied catalyst potential vs time at different reaction temperatures and oxygen concentrations: (a) 5% O_2 and (b) 7% O_2. Total flow rate = 4 L/h.

Table 2
Influence of the oxygen concentration and reaction temperature on the promotional parameters of Pt/K-βAl_2O_3 electrochemical catalysts. Reaction conditions: $[C_3H_6] = 2000$ ppm, $[O_2] = 5$–7%, He balance, total flow rate = 4 L/h

	Temperature (°C)	220	230
5% O_2	ρ	1.94	2.30
	γ	1.00	2.40
	Temperature (°C)	190	200
7% O_2	ρ	2.10	7.00
	γ	1.00	7.00

concentrations and reaction temperatures. Table 2 summarizes the influence of the oxygen concentration and reaction temperature on the promotional parameters. It can be observed that the catalyst can be strongly promoted under oxygen-rich conditions; for instance, under C_3H_6/O_2: 2000 ppm/7%, at 200 °C (Fig. 8b), propene conversion was strongly increased by application of $V_{WR} = -2$ V. Even though the temperature was quite low, a very high conversion (70%) was obtained together with a high rate enhancement ratio ($\rho_{CO_2} = 7$). This is the first time that such large promotional phenomenon has been found for propene combustion under an excess of oxygen using a Pt-based electrochemical catalyst. Previous studies have found that electropumping Na ions from Na-βAl_2O_3 [10] or NASICON [11] can activate Pt catalysts for propene oxidation under fuel-rich conditions. Nevertheless, under oxygen-rich conditions, as in exhaust gases, the electrochemical supply of ions decreases the catalytic activity. Such different behavior under oxygen-rich conditions could be attributed to both the different oxygen/propene ratios and the higher reaction temperatures used in these previous studies, for example, 340 °C for Pt/Na-βAl_2O_3 [10] and 300 °C for Pt/NASICON [11] compared with the 230 °C used in the present study. Dorado et al. [28] reported that an increase in the reaction temperature leads to an increase in the relative coverage between oxygen and propene ($\theta_O/\theta_{C_3H_6}$), changing the potentiostatic behavior of the electrochemical catalyst. On the other hand, using a Pt/YSZ electrochemical catalyst, Kaloyannis and Vayenas [8] found a high promotional effect ($\rho = 6$) for propene combustion under oxygen-rich conditions, but at a very high temperature (350–480 °C). The use of Pt/K-βAl_2O_3 electrochemical catalyst shows potential for the practical application of EPOC for the removal of VOCs, because the system can be electrochemically promoted under excess of oxygen at very low temperatures (e.g., at 200 °C under 7% O_2). Under such reaction conditions, the unpromoted catalyst ($V_{WR} = 2$ V) is covered mainly by propene or by propene-derived carbonaceous species, preserving a low conversion (low temperature). A decrease in catalyst potential strongly enhances the propene oxidation rate by promoting oxygen adsorption. Furthermore, a permanent NEMCA effect is clearly observed. Thus, values of $\gamma = 2.4$ and 7 were found at 230 and 200 °C for an oxygen concentration of 5 and 7%, respectively (Table 2).

We analyze the origin of this permanent NEMCA effect out in the next section. However, from Tables 1 and 2, two general trends can be anticipated with increasing oxygen concentration in the feed: (i) the permanent NEMCA effect becomes more pronounced, and (ii) the permanent NEMCA effect occurs at lower reaction temperatures.

3.4. Investigations of the origin of the NEMCA effect

3.4.1. Cyclic voltammetry measurements

To investigate the origin of the permanent NEMCA effect, cyclic voltammetry was carried out in conjunction with CO_2 analysis under near-stoichiometric conditions at 250 and 290 °C (Fig. 9). As reported in previous studies for Na^+-conducting electrolytes [11,12], the observed cathodic and anodic peaks were directly linked to the back-spillover of ions between the solid electrolyte and the catalyst surface, which led to the electron charge-transfer reaction between the ions and the different species adsorbed on the catalyst surface. At 250 °C (Fig. 9a), a reversible promotional phenomenon was found during cyclic voltammetry, due to the formation (cathodic peak) and decomposition (anodic peak) of a potassium surface compound as a consequence of the negative and positive polarization, respectively. Based on the area of the cathodic peak and the Faraday's law, a potassium promoter coverage of 0.7% on Pt can be estimated. Taking into account the composition of the feed, the potassium compound may be considered to be potassium carbonate, as was previously detected by XPS under similar reaction conditions [23]. Nevertheless, due to the formation of H_2O, we cannot rule out the formation of potassium

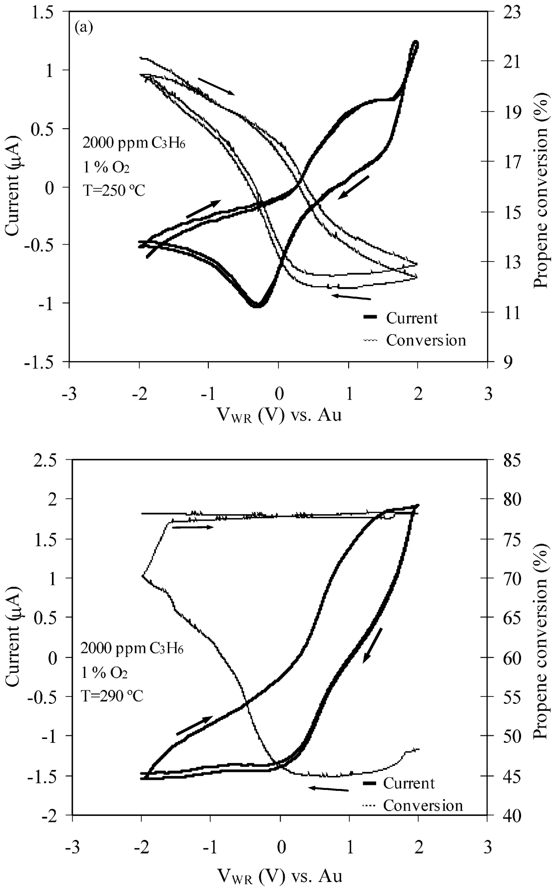

Fig. 9. Propene conversion and current vs catalyst potential (V_{WR}) during cyclic voltammetry under reaction conditions at different reaction temperatures. Total flow rate = 4 L/h, scan rate: 2 mV/s.

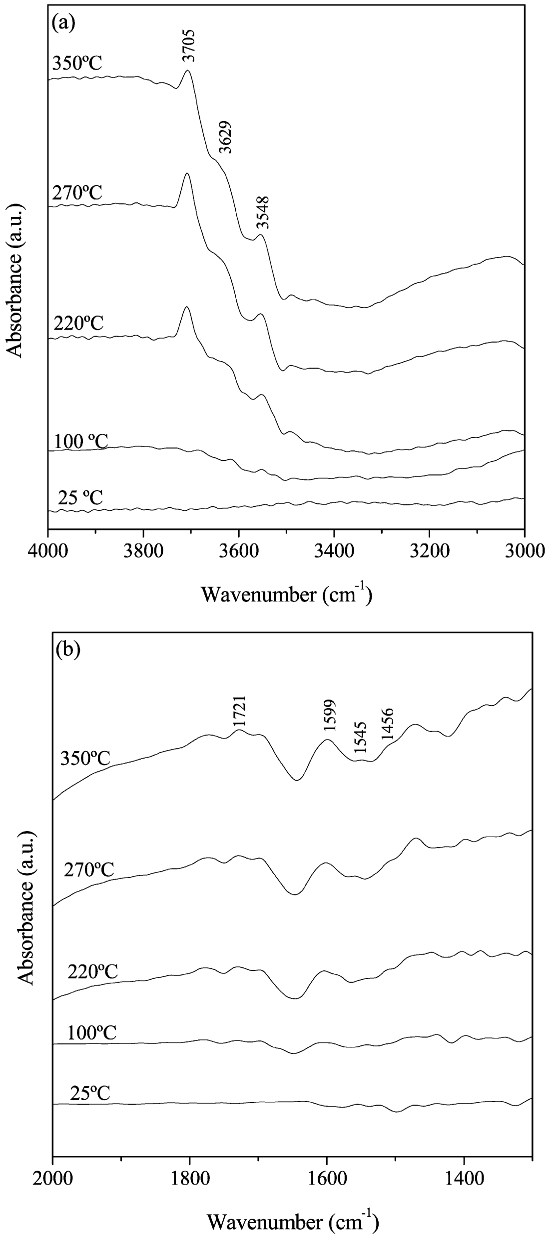

Fig. 10. FTIR spectra of adsorbed species on 1% Pt/K-βAl_2O_3 at different reaction temperatures. Reaction conditions: $[C_3H_6] = 2000$ ppm, $[O_2] = 1\%$, He balance, total flow rate = 4 L/h.

bicarbonate, as has already been deduced with sodium conductors [11].

On the other hand, at 290 °C (Fig. 9b), a permanent NEMCA effect was observed during cyclic voltammetry. At the same time, a widening (probably due to the appearance of a second peak on both the cathodic and anodic regions) and an increasing intensity of the voltammetry peaks also could be observed. This seems to indicate that at 290 °C, additional promoter species were formed during negative polarization (i.e., increased potassium promoter coverage to 1.5%) that were not totally decomposed during positive polarization (i.e., widening of the anodic peak). Therefore, we can suggest that as the reaction temperature increased, the formation of additional and more stable potassium promoter species occurred, leading to the observed permanent NEMCA effect. We could envisage that possible candidates could be potassium oxide or superoxide phases, because potassium peroxy or superoxy potassium compounds have been detected over Ag/K-βAl_2O_3 electrochemical catalyst under similar reaction conditions [34].

3.4.2. FTIR measurements

To identify the chemical state of the different potassium promoter species on the catalyst surface, FTIR measurements were carried out under different reaction conditions over 1% Pt/K-βAl_2O_3 catalyst powder. The Pt active phase dispersed on the K-βAl_2O_3 support was already promoted before the FTIR analysis, due to the thermal migration of potassium ions from the support to the Pt particles during the preparation step. Therefore, the 1% Pt/K-βAl_2O_3 catalyst powder simulated the Pt catalyst working electrode of the Pt/K-βAl_2O_3 electrochemical catalyst under promoted conditions. Fig. 10 shows the FTIR spectra collected during exposure of the catalyst powder to a mixture of C_3H_6/O_2: 2000 ppm/1% at different reaction temperatures. Backgrounds were obtained at each temperature with the sample in place. Therefore, the final spectra show only the adsorbed species. The FTIR spectra were divided into two regions: 4000–3000 cm^{-1} (Fig. 10a) and 2000–1300 cm^{-1} (Fig. 10b). It can be seen that no IR bands were present below the temperature at which the conversion of propene started

(220 °C). Nevertheless, as the reaction temperature increased, IR bands of adsorbed species on the Pt/K-βAl$_2$O$_3$ catalyst were observed. Fig. 10a clearly shows several bands in the hydroxyl region (3705–3500 cm^{-1}) [35] at, for example, 3705, 3629, and 3548 cm^{-1}. According to Iordan et al. [36], the band at 3705 cm^{-1} has been related to type IIA alumina hydroxyls, or most probably AlOHK species. It is interesting to note that an increment in the reaction temperature from 220 to 270 °C led to a higher intensity of the 3705-cm^{-1} band. Nevertheless, at 350 °C, the intensity of the band decreased. Previous studies [37] have shown that at certain reaction temperatures, AlOHK species can be transformed into potassium oxides and superoxides. Thus, it can be suggested that the decreased intensity of the band at 3705 cm^{-1} could be due to the formation of potassium oxides and superoxides. Accurately determining the exact stoichiometry of the oxide or superoxide is difficult (with K_2O the leading candidate), although the adsorption of a single oxygen atom onto K_2O would lead to potassium peroxide, K_2O_2 [37]. On the other hand, several bands with increasing intensity with temperature can be seen in Fig. 10b. The band at 1721 cm^{-1} can be assigned to ν(C=O) [38,39], whereas bands in the range 1400–1600 cm^{-1} are often assigned to carbonaceous species [35,40,41]. Thus, the band at 1599 cm^{-1} was assigned to carboxylate ion CO_2^-, the band at 1545 cm^{-1} was assigned to a chelating bidentate potassium carbonate, and the band at 1456 cm^{-1} was assigned to CO_2 asymmetric stretch in potassium bicarbonate. Thus, we can confirm the presence of a wide variety of potassium promoter phases on the catalyst surface under reaction conditions. Nevertheless, the formation of additional promoter species in cyclic voltammetry at 290 °C, which produced the permanent NEMCA effect, seems to be related to the aforementioned formation of potassium oxides and superoxides above 270 °C. This would be in agreement with previous studies by Comninellis and co-workers of IrO_2/YSZ electrochemical catalyst [33,42] that found strong evidence indicating that the permanent NEMCA effect was due to the electrochemical creation and stabilization of promoter superoxides on the catalyst surface. The formation of such oxides and superoxides from the interaction between potassium ions and the oxygen adsorbed on the catalyst surface also has been reported for Ag/K-βAl$_2$O$_3$ electrochemical catalyst [34]. In our case, this interaction likely led to formation of the observed AlOHK species, which were further transformed into potassium oxides and superoxides at sufficiently high temperatures. This would explain why for a given O_2 concentration, the permanent NEMCA effect appeared above a specific reaction temperature. Under a C_3H_6/O_2 atmosphere, the O coverage on the catalyst surface increased with the reaction temperature [43], facilitating the formation of AlOHK species. On the other hand, if the oxygen concentration in the feed were increased (higher O coverage), the temperature to get a permanent NEMCA effect would be lower and this effect would be more pronounced, in agreement with the experimental results (see Tables 1 and 2).

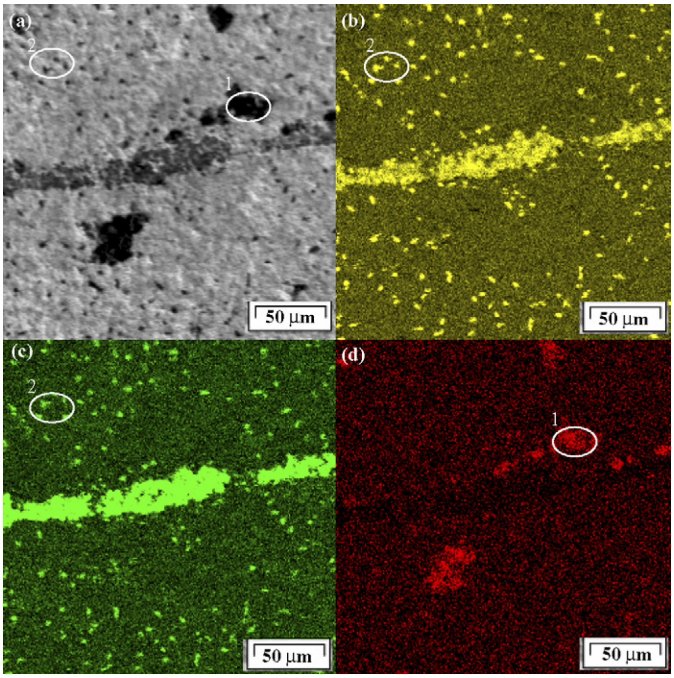

Fig. 11. SEM micrograph of (a) Pt film, and X-ray mapping of (b) potassium, (c) oxygen, and (d) carbon.

3.4.3. SEM-EDX analysis

The presence of potassium oxides and superoxides was confirmed by SEM-EDX analysis carried out over the sample after catalysis. Before the SEM-EDX analysis, the sample was kept under the following reaction conditions: C_3H_6/O_2: 2000 ppm/1% at 310 °C for 12 h, under application of $V_{WR} = -2$ V, to favor the formation of promoter species. Fig. 11 shows a SEM micrograph of the Pt film (Fig. 11a) along with a mapping of the same region for several elements: potassium (Fig. 11b), oxygen (Fig. 11c), and carbon (Fig. 11d). The Pt film (lighter color) covered most of the SEM image apart from a large central band, which shows part of the solid electrolyte. On the other hand, several darker regions can be distinguished. These darker regions were attributed to the presence of different phases formed during the catalytic experiments, because they were not observed for the fresh sample (not shown).

From the mapping of the elements (Figs. 11b–11d), two regions can be clearly distinguished in the analysis of the Pt film: region 1, formed exclusively by carbon, and region 2, formed by potassium and oxygen. Region 1 is a consequence of carbon deposition during the catalytic experiment, whereas region 2 exhibits the presence of potassium oxides and superoxides, in good agreement with the FTIR measurements. Nevertheless, the presence of potassium carbonate and bicarbonate was not observed by SEM-EDX analysis. These phases likely disappeared during the cooling period, because they seem to be less stable. Indeed, these phases were removed during the catalytic experiments under application of $V_{WR} = 2$ V, leading to a reversible promotional effect. In contrast, the potassium oxides and superoxides seem to be more stable phases, and their presence could induce the observed permanent NEMCA effect, because they may not have been completely removed under application of $V_{WR} = 2$ V. In addition, it should be noted that the higher the oxygen concentration in the feed, the greater the increase in promotional parameters (Tables 1 and 2). Therefore, the promotional effect was greater for the oxides/superoxides than for the carbonate/bicarbonate, in agreement with the two regions previously observed in Fig. 6. This should explain why under certain reaction conditions, a slight increase in catalytic activity was observed when the negative polarization was stopped (Figs. 7 and 8). This could be related to the removal of the less stable promoter phase from the catalyst. As reported previously [10,11] the growth of three-dimensional carbonate phases blocks catalyst active sites, leading to poisoning behavior. Consequently, when both promoter phases coexisted on the catalyst surface, removal of the less stable and less active phase (the carbonate/bicarbonate) would involve an additional increase in catalytic activity, because the loss of promoter was compensated for by the unblocking of Pt active sites. This can explain why we found a permanent rate enhancement ratio (γ) higher than the rate enhancement ratio (ρ) for the experiment with $[O_2] = 5\%$ at 230 °C (Table 2). In addition, it also can explain why, when using K-βAl_2O_3 as a solid electrolyte, we did not observe poisoning behavior, in comparison with sodium conductors [10,11] under near-stoichiometric oxygen conditions. With K-βAl_2O_3, part of the promoter phase is a potassium oxide/superoxide. This compound seems to induce a promoting effect greater than the inhibiting effect. The observed strong permanent NEMCA effect has not been shown in previous studies on propene combustion over Pt/Na-βAl_2O_3 [10] or Pt/NASICON [11] electrochemical catalysts, where the presence of such oxides/superoxides was not detected. It could be attributed to the smaller Pt particle size in the Pt film prepared in this work by the wet-impregnation procedure, along with the greater electronic effect of potassium ions. The combination of these two factors can allow the formation of the stable and effective potassium oxide/superoxide promoters. As mentioned above, potassium increased the oxygen coverage on the catalyst surface more strongly than sodium [29]. It is likely that the formation of the stable oxide/superoxide promoters cannot occur when sodium conductors are used as solid electrolytes.

4. Conclusion

This work has produced numerous findings regarding the characterization and catalytic properties of Pt/K-βAl_2O_3 electrochemical catalysts for low-temperature propene combustion. Surface titration, XRD, and SEM characterizations revealed useful information on the Pt catalyst film, showing a porous morphology with a metallic dispersion of 5%, similar to that observed for the active phases deposited on a monolith configuration. Furthermore, the Pt film prepared by the deposition of a Pt precursor solution exhibited significant resistance to thermal sintering, as well as a small particle size, making it effective at low temperatures.

Use of the Pt/K-βAl_2O_3 electrochemical catalyst points up the practical applications of EPOC for the catalytic combustion of hydrocarbons. It was found that Pt/K-βAl_2O_3 electrochemical catalyst can be strongly promoted at low temperature and demonstrates good catalytic performance under both near-stoichiometric and oxygen-rich conditions. In addition, the identification of potassium promoter species under reaction conditions has established the origin of the observed permanent NEMCA effect. The use of cyclic voltammetry in conjunction with CO_2 analysis, FTIR measurement, and SEM-EDX analysis clearly show that this phenomenon was due to the formation of additional, more stable and effective potassium promoter phases: potassium oxides and superoxides. The presence of such phases also may have been responsible for the greater promotion with no poisoning found in the present study in comparison with previous studies using sodium conductors.

Acknowledgments

Financial support was provided by the Ministerio de Educación y Ciencia of Spain (Project CTQ2004-07350-C02-01/PQ) and University Claude Bernard Lyon 1 (Bonus Qualité Recherche). Antonio de Lucas-Consuegra received an FPU grant from the Spanish Government for financial support during his stay in IRCELYON. The two laboratories involved in this research are members of the European Marie-Curie EFE-POC project "European Forum on Electrochemical Promotion of Catalysis" (contract MSCF-CT-2006-046201).

References

[1] R. Burch, M.J. Hayes, J. Mol. Catal. A 100 (1995) 13.

[2] M. Stoukides, C.G. Vayenas, J. Catal. 70 (1981) 137.

[3] C.G. Vayenas, S. Bebelis, S. Ladas, Nature (London) 343 (1990) 625.

[4] C.G. Vayenas, S. Bebelis, C. Pliangos, S. Brosda, D. Tsiplakides, Electrochemical Activation of Catalysis, Kluwer Academic/Plenum, New York, 2001.

[5] C.G. Vayenas, S. Bebelis, I.V. Yentekakis, H.-G. Lintz, Catal. Today 11 (1992) 303.

[6] I.V. Yentekakis, G. Moggridge, C.G. Vayenas, R.M. Lambert, J. Catal. 146 (1994) 292.

[7] P. Vernoux, F. Gaillard, L. Bultel, E. Siebert, M. Primet, J. Catal. 208 (2002) 412.

[8] A. Kaloyannis, C.G. Vayenas, J. Catal. 182 (1999) 37.

[9] P. Beatrice, C. Pliangos, W.L. Worrell, C.G. Vayenas, Solid State Ionics 136 (2000) 833.

[10] N.C. Filkin, M.S. Tikhov, A. Palermo, R.M. Lambert, J. Phys. Chem. A 103 (1999) 2680.

[11] P. Vernoux, F. Gaillard, C. Lopez, E. Siebert, Solid State Ionics 175 (2004) 609.

[12] F. Dorado, A. de Lucas-Consuegra, P. Vernoux, J.L. Valverde, Appl. Catal. B 73 (2007) 42.

[13] I.M. Campbell, Catalysis at Surfaces, Chapman & Hall, New York, 1988.

[14] M. Konsolakis, I.V. Yentekakis, Appl. Catal. B 29 (2001) 103.

[15] Y. Minemura, M. Kuriyama, S. Ito, K. Tomishige, K. Kunimori, Catal. Commun. 7 (2006) 623.

[16] F.J. Williams, A. Palermo, S. Tracey, M.S. Tikhov, R.M. Lambert, J. Phys. Chem. B 106 (2002) 5668.

[17] F. Dorado, A. de Lucas, P.B. García, J.L. Valverde, A. Romero, Appl. Catal. B 65 (2006) 175.

[18] S. Balomenou, D. Tsiplakides, A. Katsaounis, S. Thiemann-Handler, B. Cramer, G. Foti, Ch. Comninellis, G.C. Vayenas, Appl. Catal. B 52 (2004) 181.

[19] J. Dawody, M. Skoglundh, S. Wall, E. Fridell, J. Mol. Catal. A 225 (2005) 259.

[20] G. Fóti, S. Wodiuning, Ch. Comninellis, Curr. Top. Electrochem. 7 (2000) 1.

[21] G. Fóti, I. Bolzonella, J. Eaves, Ch. Comninellis, Chimia 56 (2002) 137.

[22] A.J. Urquhart, F.J. Williams, R.M. Lambert, Catal. Lett. 103 (2005) 137.

[23] A.J. Urquhart, J.M. Keel, F.J. Williams, R.M. Lambert, J. Phys. Chem. B 107 (2003) 10591.

[24] R.M. Lambert, A. Palermo, F.J. Williams, M.S. Tikhov, Solid State Ionics 136 (2000) 677.
[25] G. Pitselis, P. Petrolekas, C.G. Vayenas, Ionics 3 (1997) 110.
[26] R.T. Baker, Carbon 27 (1989) 315.
[27] S. Bernard, L. Retailleau, F. Gaillard, P. Vernoux, A. Giroir-Fendler, Appl. Catal. B 55 (2005) 11.
[28] F. Dorado, A. de Lucas-Consuegra, C. Jiménez, J.L. Valverde, Appl. Catal. A 321 (2007) 86.
[29] N.D. Lang, S. Holloway, J.K. Norskov, Surf. Sci. 150 (1985) 24.
[30] I.V. Yentekakis, R.M. Lambert, M. Tikhov, M. Konsolakis, V. Kiousis, J. Catal. 176 (1998) 82.
[31] M. Konsolakis, I.V. Yentekakis, A. Palermo, R.M. Lambert, Appl. Catal. B 33 (2001) 293.
[32] A. Billard, P. Vernoux, Top. Catal. 44 (2007) 369.
[33] E. Varkaraki, J. Nicole, E. Plattner, C. Comninellis, J. Appl. Electrochem. 25 (1995) 978.
[34] A. Palermo, A. Husain, M.S. Tikhov, R.M. Lambert, J. Catal. 207 (2002) 331.
[35] T.J. Toops, D.B. Smith, W.S. Epling, J.E. Parks, W.P. Partridge, Appl. Catal. B 58 (2005) 255.
[36] A. Iordan, M.I. Zaki, C. Kappenstein, J. Chem. Soc. Faraday Trans. 89 (1993) 2527.
[37] T.J. Toops, D.B. Smith, W.P. Partridge, Catal. Today 114 (2006) 112.
[38] M. Xin, I.C. Hwang, S.I. Woo, Catal. Today 38 (1997) 187.
[39] K. Shimizu, A. Satsuma, T. Hattori, Appl. Catal. B 25 (2000) 239.
[40] G.R. Bamwenda, A. Ogata, A. Obuchi, J. Oi, K. Mizuno, J. Skrzypek, Appl. Catal. B 6 (1995) 311.
[41] M. Xin, I.C. Hwang, S.I. Woo, J. Phys. Chem. B 101 (1997) 9005.
[42] D. Tsiplakides, J. Nicole, C.G. Vayenas, C. Comninellis, J. Electrochem. Soc. 145 (1998) 905.
[43] X. Li, F. Gaillard, P. Vernoux, Ionics 11 (2005) 103.